Journal of *Marine Science and Engineering*

MDPI

Article

Design and Development of an SVM-Powered Underwater Acoustic Modem

Gabriel S. Guerrero-Chilabert [1,*,†], David Moreno-Salinas [1,†] and José Sánchez-Moreno [1,†]

Department of Computer Science and Automatic Control, Universidad Nacional de Educación a Distancia (UNED), Juan del Rosal 16, 28040 Madrid, Spain; dmoreno@dia.uned.es (D.M.-S.); jsanchez@dia.uned.es (J.S.-M.)

* Correspondence: gguerrero16@alumno.uned.es

† These authors contributed equally to this work.

Abstract: Underwater acoustic communication is fraught with challenges, including signal distortion, noise, and interferences unique to aquatic environments. This study aimed to advance the field by developing a novel underwater modem system that utilizes machine learning for signal classification, enhancing the reliability and clarity of underwater transmissions. This research introduced a system architecture incorporating a Lattice Semiconductors FPGA for signal modulation and a half-pipe waveguide to emulate the underwater environment. For signal classification, support vector machines (SVMs) were leveraged with the continuous wavelet transform (CWT) employed for feature extraction from acoustic signals. Comparative analysis with traditional signal processing techniques highlighted the efficacy of the CWT in this context. The experiments and tests carried out with the system demonstrated superior performance in classifying modulated signals under simulated underwater conditions, with the SVM providing a robust classification despite the presence of noise. The use of the CWT for feature extraction significantly enhanced the model's accuracy, eliminating the need for further dimensionality reduction. Therefore, the integration of machine learning with advanced signal processing techniques presents a promising research line for overcoming the complexities of underwater acoustic communication. The findings underscore the potential of data mining methodologies to improve signal clarity and transmission reliability in aquatic environments.

Keywords: underwater acoustic communication; signal processing; support vector machines; continuous wavelet transform; FPGA; feature extraction; modulation techniques; noise reduction

Citation: Guerrero-Chilabert, G.S.; Moreno-Salinas, D.; Sánchez-Moreno, J. Design and Development of an SVM-Powered Underwater Acoustic Modem. *J. Mar. Sci. Eng.* **2024**, *12*, 773. https://doi.org/10.3390/jmse12050773

Academic Editor: Dong-Sheng Jeng

Received: 5 April 2024
Revised: 29 April 2024
Accepted: 3 May 2024
Published: 5 May 2024

1. Introduction

Underwater acoustic (UWA) communication is a pivotal area of research, driven by its critical applications in underwater exploration, surveillance, and data transmission between submerged devices. Despite its importance, the field faces significant challenges, including signal attenuation, multipath propagation, and noise interferences, which severely impact the reliability and clarity of underwater transmissions [1].

These unique challenges are due to the inherent properties of the aquatic environment, such as significant signal distortion and persistent noise from various natural and anthropogenic sources, such as ocean currents, marine life, vessel propellers, and the relative movement of communicating parties, each introducing their own complexities to signal transmission and reception [2]. Addressing these challenges, this work introduced a new approach that leverages a combination of the continuous wavelet transform (CWT) and support vector machines (SVMs) for the effective demodulation of known frequency shift keying (FSK) signals.

The current state of research in UWA communication reveals a spectrum of approaches, from traditional signal processing methods to emerging machine learning algorithms. While traditional techniques have provided a foundation for the field, they often fall short in complex scenarios characterized by variable noise conditions and dynamic aquatic

environments. In order to mitigate these harsh conditions, several approaches have been adopted. In [3], a compressed sensing-based technique for time-domain synchronization is proposed over a real-time underwater channel. In [4], a new estimation scheme, which does not suffer from intercarrier interference (ICI), is proposed to estimate the channel variations. In [5], a precoded index modulation is proposed to increase the transmission efficiency and exploit the spreading and multipath diversities.

These complex underwater conditions have led to a growing interest in data-driven approaches, which offer adaptability and improved performance. In this sense, recent advancements have leveraged sophisticated signal-processing techniques and machine learning to enhance communication capabilities in these challenging environments. For example, the work described in [6] employed a neural network with feature extraction and automatic learning ability to replace the demodulation modules to recover transmitted signals without explicit channel estimation and equalization. A UWA communication modulation classifier is proposed in [7], which uses a convolutional neural network (CNN) to identify the presence of the UWA signals; then, the classifier uses the feature vector output by the encoder to distinguish the final modulation categories. Other interesting examples are found in [8–10]. In [8] an SVM classifier is employed, along with a CNN in a camera receiver. A CNN is used to detect every LED region from the image frame, and then essential features are extracted to feed into an SVM classifier for further accurate classification. In [9], a Q-learning-based adaptive switching scheme to maximize the network throughput by capturing the dynamics of the varying channels was developed. In [10], neural network architectures and training methods suitable for demodulation in power-limited communication systems were examined.

Among the different approaches, the SVM and CWT have emerged as promising tools for improving signal classification and feature extraction, respectively [11–13]. However, the integration of these techniques in underwater communication systems, particularly in conjunction with FPGA-based architectures for real-time processing, remains underexplored. Some exceptions that employ this FPGA-based architecture are found in [14,15]. The research described in [14] implemented and tested an SVM classifier on an FPGA, where a discrete wavelet transform (DWT) was used to extract the features of received modulated signal, and depending on these features, an SVM can classify binary phase shift keying (BPSK) and quadrature phase shift keying (QPSK) modulation techniques. The authors in [15] proposed an FPGA-based achitecture to embody several modulation techniques at once, making it more versatile, cost-effective, and easy to use and test.

In addition, some works have developed systems and methodologies for the modulation and/or demodulation of acoustic and optical signals in the underwater environment using machine learning techniques. For example, an asymmetric frequency shift keying (AFSK) modulation technique for visible light communication (VLC) systems was developed in [16]. AFSK provides VLC systems with a low-cost and low-complexity modulation technique that mitigates flickering and dimming for both square and rectified sine wave signals. The authors in [17] used a deep convolutional neural network (DCNN) for the demodulation of a Rayleigh-faded wireless data signal, simulating the FSK demodulation over an additive white Gaussian noise Rayleigh fading channel with average signal-to-noise ratios (SNRs) from 10 dB to 20 dB. In [18], a single deep learning (DL) model to demodulate the ASK, FSK, and PSK modulations by using a data-driven approach is presented. The research in [19] presents two DL-based demodulators called a deep belief network support vector machine (DBN-SVM) demodulator and adaptive boosting (AdaBoost)-based demodulator. The work [20] shows a modulation recognition method based on time–frequency analysis and an SVM. Ref. [21] proposes an optimization algorithm based on instantaneous statistical characteristics of modulated signals and an SVM classifier. In [22], a modulation classification method capable of classifying multiple FSK digital signals without a priori information using modified covariance method was developed. However, as far as the authors know, there does not exist a similar approach to the one presented in this work,

in which the signal modulation/demodulation is made by the combination of SVM, CWT, and FSK methods and implemented in an FPGA-based architecture.

Therefore, this work aimed to address this gap by developing an advanced underwater acoustic modem system that employs SVM for signal classification and the CWT for feature extraction. Unlike conventional research that primarily focuses on signal type identification, the method presented utilizes these advanced techniques to accurately decode signals and retrieve transmitted data under simulated underwater conditions. The modem employs FSK modulation for transmitting data and utilizes a combination of wavelet processing and a trained SVM model for demodulation in order to demonstrate the efficacy of an SVM-based classification system integrated with the CWT for feature extraction in a custom-designed FPGA-based underwater modem. The introduction of a new symbol named "C" in the decoding process allows for a more flexible interpretation of the signal transitions, enhancing the robustness and accuracy of data demodulation. This symbol acts as a transitional element within the signal structure, aiding in the mitigation of common issues, such as spectrum leakage and transition errors, that are typically encountered in underwater communications. Through experimentation and analysis, this study contributes to the theoretical understanding of machine learning applications in signal processing and also provides a practical framework for enhancing underwater communication systems.

In addition, the approach proposed not only applies SVM in a novel context but also demonstrates the superiority of the CWT over traditional Fourier-based methods for handling the dynamic aspects of underwater acoustics. The integration of these techniques into the modem design offers a more reliable and efficient method for underwater communication that exceeds the capabilities of conventional systems.

The subsequent sections detail the system architecture, experimental setup, and performance outcomes, underscoring the transformative potential of the approach presented in the realm of underwater acoustic communication. In Section 2, the software and hardware tools, as well as the methodology followed, are detailed. In Section 3, the main outcomes obtained showing the effectiveness of the system are described. In Section 4, the results and methods are discussed, and the final conclusions are drawn in Section 5, which also indicates future lines of research.

2. Materials and Methods

This study employed a comprehensive suite of hardware and software tools to develop and evaluate an advanced underwater acoustic modem system leveraging an SVM for signal classification and the CWT for feature extraction. These tools, as well as the methodology followed for the construction and test of the prototype, are described next. The experimental results presented in this paper were obtained under controlled laboratory conditions designed to emulate the underwater acoustic environment.

2.1. Hardware Setup

The core of the experimental setup is a Lattice Semiconductors ICE5LP1K FPGA, which was used for signal modulation and processing. This FPGA was selected for its low power consumption and sufficient logic element capacity to handle the required processing tasks. The FPGA was programmed in Verilog to perform the FSK modulation. This involved generating precise control signals to drive the high-voltage oscillator, which, in turn, excited the PZT4 ultrasonic transducer for signal transmission. Custom-designed PCBs facilitated the integration of the FPGA with other hardware components, including the high-voltage signal generator for the transmitter and a specialized filter and amplifier circuit for the receiver.

Then, the data source for the experiments was an FSK modulator, which consisted of a 200 kHz PZT4 transducer equipped with a high-voltage oscillator for the excitation. The choice of these transducers was based on their frequency response, aligning with the target communication frequencies. The control of this oscillator was mediated through high-power MOSFET transistors governed by the FPGA programmed to produce the required FSK modulation. An example of the resultant modulated signal is shown in Figure 1a.

The experimental setup was constructed to mimic the constraints of an underwater communication channel. The signal transmission was conducted through a 6 m waveguide, which served as a controlled medium to replicate the acoustic properties of an underwater environment. This approach allowed for the precise manipulation and measurement of the acoustic signals, thus ensuring the reliability of the data for subsequent digital processing.

Data acquisition and signal monitoring were performed using a Fluke 190-504 (FLUKE, Everett, WA, USA) Scopemeter Series III and a Rigol MSO5354 (RIGOL, Gilching, Germany) digital oscilloscope, which ensured high-fidelity capture of the transmitted and received signals. To capture the transmitted signals, the oscilloscopes were set at both the transmitter and receiver ends. The Fluke and Rigol oscilloscopes used in the experiments were capable of high-resolution measurements, capturing the signal at a rate of 8 GSPS, which was then decimated to 2 MSPS to suit the system's requirements. The oscilloscopes facilitated an accurate data acquisition process that was fed into MATLAB scripts for further processing and analysis.

To maintain the integrity of the signals and to negate the influences of variable laboratory conditions, such as temperature fluctuations and extraneous noise, stringent controls were imposed. While acknowledging the deviation from open-sea trials, these laboratory conditions offered a rigorous and stable testing environment for ascertaining the performance of the underwater modem system. The fidelity of these conditions to actual underwater scenarios was anticipated to provide a robust indication of the system's operational efficacy in situ. The system was set up as follows:

- The FPGA board was connected to the transmission board via a board-to-board connector.
- The transmission board was linked to the ultrasonic transducer PZT4.
- The Fluke 190-504 CH1 was connected to the signal input from the FPGA in the transmission board.
- The Fluke 190-504 CH2 was connected to the PZT4 transmission transducer to monitor the exact transmitted signal.
- The Rigol MSO5354 CH1 was connected to the output of the filter + amplifier block.
- The Rigol MSO5354 CH3 was connected to the PZT4 receiver transducer for system troubleshooting.

For the system setup and verification, the CH1 and CH3 channels of the Rigol oscilloscope were enabled. The trigger was set to CH3, AC coupled, and given a rising edge in normal mode, resulting in a sampling rate of 2 GSPS. For the signal gathering, only CH1 was enabled, with the trigger set to CH1, AC coupled, given a rising edge, and in SINGLE mode. The acquisition memory depth was set to 200 Mpts, enabling the scope to sample at 8 GSPS. In Figure 1b, a closeup of the scope (Fluke) with three signals is shown. In red, the modulating signal from the FPGA is given; in dark grey, the signal on the PZT4 Transducer (Tx) is given; and in green, the signal received at the PZT4 transducer (straight from the Rx transducer) of the receiver is given. This capture was done for the sensitivity validation of the receiver transducer (no pre-amp used).

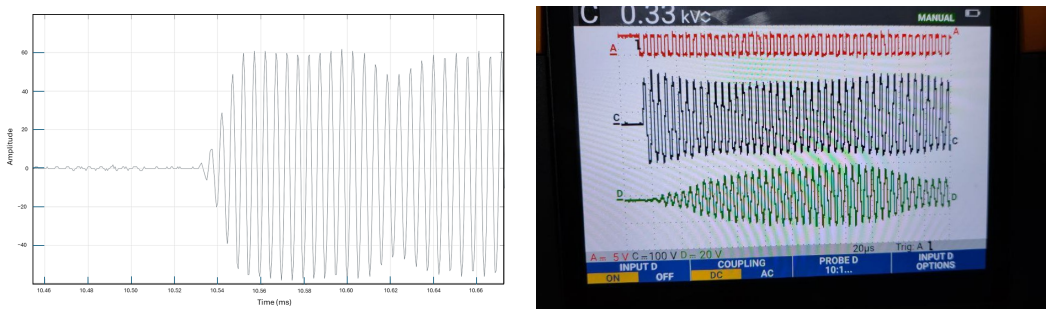

(**a**) (**b**)

Figure 1. Example of the modulated signal (**a**) and oscilloscope view of the modulated (red), transmitted (dark grey), and received (green) signals (**b**).

The design concept and setup are shown in Figure 2.

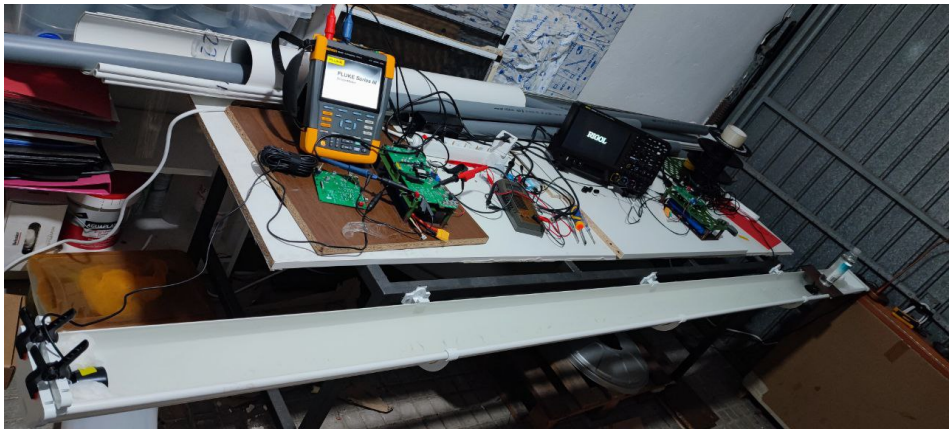

Figure 2. The hardware setup.

2.2. Software Tools

Signal processing and classification were carried out using MATLAB, with custom scripts developed for data decimation, feature extraction using the CWT, and SVM classification.

For the feature extraction, the CWT was utilized by leveraging the "bump" wavelet, which is preferred for its robust response to non-stationary signals in noisy environments. The CWT's ability to localize signal characteristics in both the time and frequency domains makes it particularly suitable for analyzing the complex signals encountered in underwater acoustic communication. The mathematical details of the CWT and the reasons for choosing the "bump" wavelet are expounded in Sections 3 and 4, respectively, with comparative analyses highlighting its advantages over the FFT and STFT in extracting meaningful features from acoustic signals.

The SVM classifier was configured with a radial basis function (RBF) kernel, which is ideal for handling the nonlinearities in the feature space created by the CWT. Parameter tuning, particularly for the **C** and γ parameters of the SVM, was conducted through a series of validation tests to enhance the classification accuracy.

The MATLAB environment was also used for the initial data processing and visualization, including the generation of scalograms and the plotting of signal characteristics.

For the development and synthesis of the FPGA's Verilog code, the iCEcube2 Version 2020.12 software (Lattice Semiconductors, Hillsboro, OH, USA) suite was utilized, which allowed for precise control over the FPGA's functionality and signal-processing capabilities.

2.3. Methodology and Data Analysis

The study methodology encompassed the design, implementation, and evaluation of the underwater modem system. This involved the following:

1. Programming the FPGA to modulate input signals using FSK modulation.
2. Emitting modulated signals through the underwater waveguide using the transmitter setup.
3. Receiving and processing these signals at the receiver end to extract relevant features using the CWT.
4. Classifying the received signals based on the extracted features using an SVM model trained on predefined signal patterns.

New methods and protocols introduced in this study, such as specific configurations of the FPGA for underwater signal generation, scripts, and the application of the CWT for feature extraction in an aquatic environment, are detailed in the supplementary materials available upon request to the authors. Established methods, such as SVM classification, are described in accordance with the existing literature [23–25].

For data acquisition, the script establishes a connection with the Rigol oscilloscope, configures the necessary settings, and captures the waveform data. The process of analyzing and classifying signals using an SVM can be visualized as a sequential flow. The procedure begins with the raw signal, which undergoes several stages of transformation and analysis before a final prediction is made. These stages are as follows:

- Feature extraction: The raw signal, which often contains a vast amount of data, is first subjected to a feature extraction process. This step is crucial for two reasons: (i) Information retrieval: the raw signal contains a plethora of information, not all of which is relevant or useful for classification. Feature extraction aims to capture the most informative characteristics of the signal, which are indicative of its underlying patterns or behaviors. (ii) Dimensionality reduction: High-dimensional data can be computationally expensive and challenging to work with, especially in machine learning contexts. By extracting salient features, the dimensionality of the data is effectively reduced, making subsequent processes more efficient and accurate [26].
- Labeling process: Once the features are extracted, each data point (or set of features) is associated with a label. This label indicates the category or class to which the data point belongs. The labeling can be done manually, through expert knowledge, or automatically using specific algorithms.
- SVM training: With the features extracted and labeled, the SVM model is trained. During this phase, the SVM algorithm learns the boundaries and patterns within the data. It tries to find the optimal hyperplane that best separates the different classes in the feature space.
- SVM validation: After training, it is essential to validate the SVM model performance. This step involves using a separate dataset (not used during training) to test the model accuracy and robustness. Any discrepancies or issues highlighted during validation can be addressed by refining the model or revisiting the feature extraction phase.
- SVM prediction: Once validated, the SVM model is ready to make predictions on new unseen data. Given a new signal or data point, the model can now classify it based on the patterns it learned during training.

Regarding the feature extraction, the CWT was selected since it offers a very flexible approach to wavelet analysis and due to its ability to provide a time-frequency representation of the signal, which was crucial for capturing the nuances of the modulated signal [27]. Instead of using fixed and dyadic scales as in the DWT, the CWT analyzes the signal at every possible scale, providing a truly continuous transformation. This makes the CWT especially valuable for capturing transients or rapidly changing features in a signal. The CWT was explored, with various wavelets being analyzed for their suitability. Then, the final choice for feature extraction was the CWT using the "bump" wavelet. The CWT analysis focused on the band between 150 kHz and 250 kHz, excluding features outside this band from the wavelet transform; see Figure 3 for a raw scalogram before the feature selection. The colors depicted in the scalogram correspond to the amplitude or strength of the wavelet coefficients at each time and frequency location, as indicated by the color bar to the right.

In Figure 3, the vertical axis enumerates the frequency bins, where each bin represents a range of frequencies, with bin 1 corresponding to the lowest frequency range and higher bins corresponding to progressively higher ranges. These bins are integral to the feature extraction process, as they simplify the complex frequency spectrum into manageable segments for analysis by the SVM classifier. The "Frequency Bin" axis is thus a discrete index that correlates with specific frequency ranges defined by the CWT analysis, which, in this study, focused on the 150 kHz to 250 kHz band. The bins help to identify which portions of the signal spectrum are most relevant for classification and demodulation purposes. This categorization is crucial for machine learning applications, where input features must be distinctly identifiable and consistent across different instances of data.

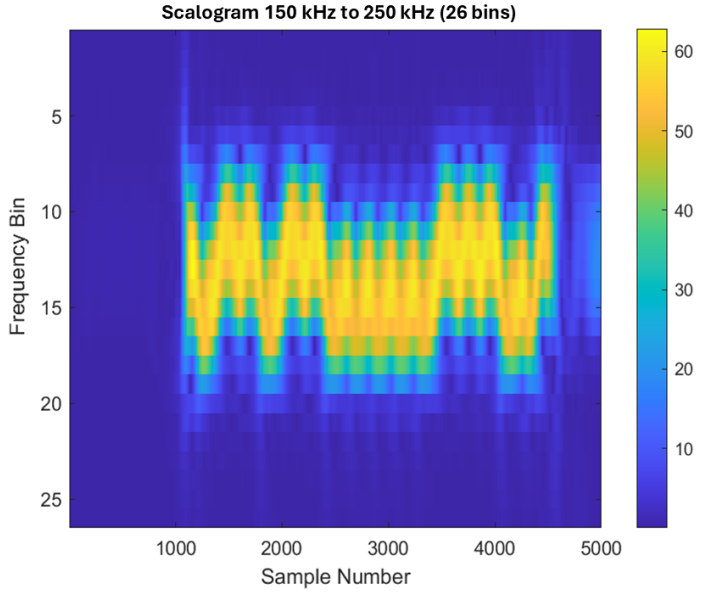

Figure 3. The 150 kHz to 250 kHz scalogram.

In the stage of preparing the dataset for supervised learning process, a meticulous labeling procedure was undertaken. The objective was to assign appropriate class labels to each of the extracted features from the CWT. Four distinct classes were chosen for labeling:

- 1: Representing the symbol "1", which was transmitted at a frequency of 205.512 kHz.
- 0: Representing the symbol "0", which was transmitted at a frequency of 185.675 kHz.
- C: Initially intended to identify the clock, this symbol was later adapted to serve as a transitional symbol between "1" and "0", and its corresponding frequency was 195.487 kHz. This decision was influenced by the challenges faced during the transmitter design and the FPGA coding in Verilog, particularly concerning the spectrum leakage and the transition difficulties. Introducing the "C" symbol between "1" and "0" symbols provided flexibility in training the SVM, allowing the "C" to be trained as "from 0 C" or "from 1 C".
- N: A generic class that represented all symbols that were neither "1", "0", nor "C".

Then, the symbols "1", "0", and "C" were emitted at a different frequency each along 20 cycles (100 µs for 200 kHz). Figure 4a,b depict the labeling process undertaken to train the SVM, showcasing the clear distinction between the classes, particularly emphasizing the "C" class. The numbers below Figure 4 represent the sample numbers, which corresponded to distinct time intervals of the modulated signal captured for the SVM classification. This numerical sequence facilitated an understanding of the temporal structure within the dataset. The labeling was executed within an Excel spreadsheet, which allowed for an organized and visual approach to this step.

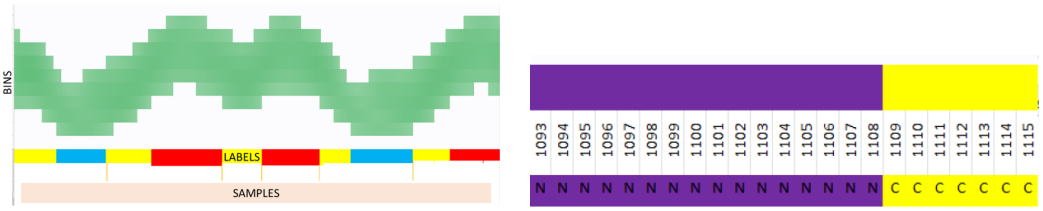

(**a**) (**b**)

Figure 4. Data labeling for training. (**a**) Zoomed-out view of the data labeling. (**b**) Detailed view of the data labeling. Numbers indicate samples.

Each class was represented by a specific color code:

- Red cells indicate the presence of the "1" symbol.
- Blue cells denote the "0" symbol.
- Yellow cells correspond to the "C" class. As indicated, this class acted as a transitional state in the modulation process and is instrumental to the method presented, ensuring a clear distinction between "1" and "0" in challenging demodulation scenarios.
- Dark violet cells were tagged as "N" for any signal that did not correspond to the defined "1", "0", or "C" symbols.

The choice of a color-coding scheme had a two-fold purpose: it expedited the labeling process and provided a quick visual reference to confirm the integrity of the labels applied to each sample. This ensured that the SVM was trained on accurately categorized data, which was crucial for the robust performance of the demodulation process. The labeling also allowed for visualizing and verifying the distribution of classes and how the features corresponding to each class manifested within the data, confirming the balanced representation of each class across the dataset. These features were derived from the CWT of the acoustic signals, encapsulating the characteristic time–frequency behavior of the transitional "C" symbol, which was central to this communication system.

The dataset was compounded of features extracted from the CWT resulting in an array of 11×5001 dimensions. Note that the CWT reduced the bins of interest to 11, as described in subsequent sections, in contrast to the 26 bins shown in Figure 3. To ensure the robustness of the SVM classifier, its performance was evaluated across different training and validation splits using K-fold cross-validation. This approach ensured that the model performance was not contingent on a specific data split, but was generally reliable.

3. Results

The following results demonstrate the effectiveness of the SVM and CWT in classifying signals for underwater acoustic communication. Detailed analysis results of the signal classification accuracy, feature extraction robustness, and system performance under varying conditions are presented, illustrating the reliability and the efficacy of the methodologies employed.

3.1. Signal Classification Accuracy

The SVM model exhibited high classification accuracy across a range of SNRs, showcasing its robustness in noisy underwater environments. The performance metrics employed were as follows:

- Accuracy across different SNRs.
- Precision and recall metrics.
- Overall system robustness.

The precision, recall, and accuracy of the signal classification model are calculated as follows:

- Precision: $\frac{\text{True Positives}}{\text{True Positives}+\text{False Positives}}$, which measures the proportion of correctly identified positive instances among all instances that were labeled as positive by the model.
- Recall: $\frac{\text{True Positives}}{\text{True Positives}+\text{False Negatives}}$, which assesses the proportion of actual positive instances that were correctly identified by the model.
- Accuracy: $\frac{\text{True Positives}+\text{True Negatives}}{\text{Total Population}}$, reflecting the overall proportion of correct predictions made by the model.

These metrics are crucial for evaluating the performance of the model, especially under varying SNR conditions in underwater communication scenarios.

The confusion matrix of the cross-validation partition of the data (remaining 20% of the data that were not used for training) is shown in Figure 5a. In addition, the precision, recall, and accuracy metrics are summarized in the aggregated confusion matrix across all SNR levels shown in Figure 5b.

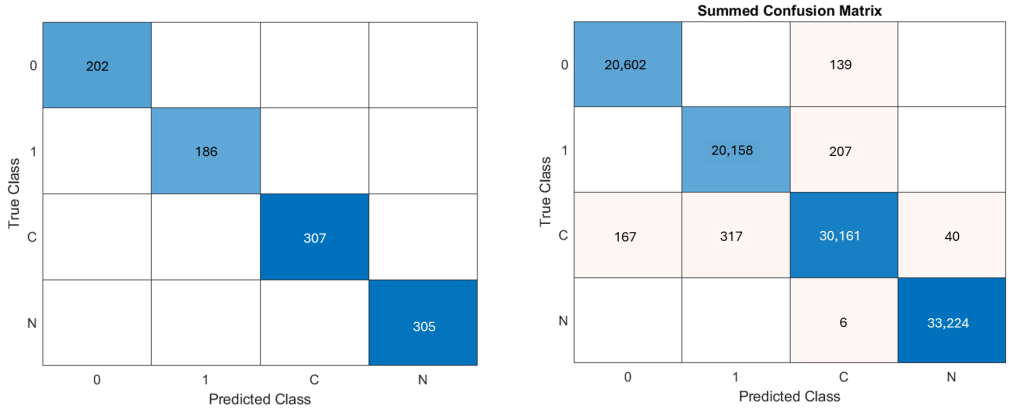

(**a**) (**b**)

Figure 5. Confusion matrices for cross-validation and training-test sets. (**a**) Confusion matrix using CV partition. (**b**) Summed confusion matrix.

The model accuracy obtained across all different SNR levels is listed in Table 1.

Table 1. Model accuracy across different SNR levels.

SNR (dB)	Accuracy
5	0.9828
6	0.9832
7	0.9832
8	0.9864
9	0.9880
10	0.9890
11	0.9906
12	0.9924
13	0.9906
14	0.9914
15	0.9936
16	0.9926
17	0.9944
18	0.9962
19	0.9964
20	0.9960
21	0.9958
22	0.9960
23	0.9978
24	0.9978
25	0.9978

The precision and recall for each class are shown in Table 2 for the best case of SNR = 25 dB. It is important to notice the high quality and precision achieved in the classification of the signals.

Table 2. Class-specific precision and recall for SNR = 25 dB.

Class	Precision	Recall
Class “0”	0.9990	0.9990
Class “1”	0.9979	0.9939
Class “C”	0.9952	0.9972
Class “N”	0.9994	1.0000

In order to highlight the good performance of the system and the model developed, the precision and recall were analyzed in deeper detail for the worst case scenario of an SNR level of 5 dB and the best case scenario of 25 dB. For this purpose, the scalogram of each case was computed due to its advantages for analyzing real-world signals with features occurring at different scales. These scalograms show the CWT of the signals as a function of the frequency for the worst case of 5 dB and best case of 25 dB in Figure 6, together with

the real signals transmitted for each case. In both cases, the features of the signals are clearly identified and are very similar despite the difference of the value of the SNR. Note that the temporal signals in Figure 6a,b are presented in milliseconds to offer a real-world temporal context to these signals, and to give a sense of the duration and timing of the signals as they occur in the physical world. The scalograms in Figure 6c,d, on the other hand, operate within the sample number domain, as this is the standard practice in signal processing for feature extraction, especially when preparing data for SVM classification. Then, these scalograms offer a visual depiction of the signal's frequency content over sample numbers, demonstrating the SVM input following the feature extraction process. The transition from milliseconds in Figure 6a,b to sample numbers in Figure 6c,d is a standard step in signal processing for feature extraction, providing the groundwork for the accurate classification by an SVM.

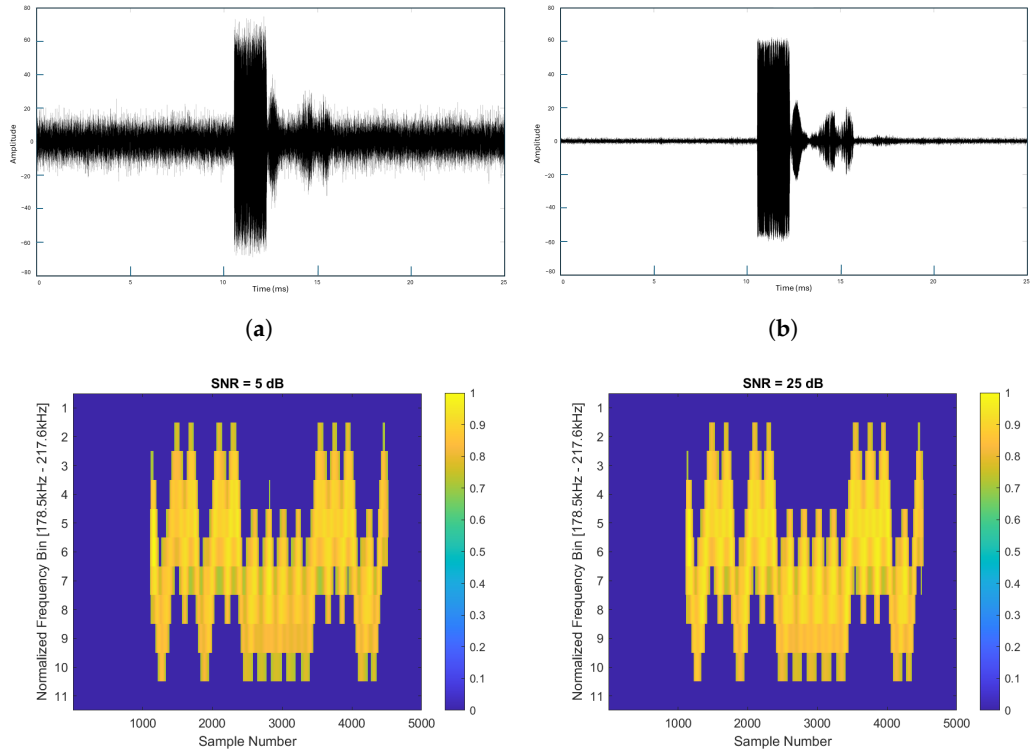

Figure 6. Noisy signals and scalograms for the worst and best SNR case scenarios. Temporal signals (**a**,**b**) depict the waveform duration in milliseconds, while scalograms (**c**,**d**) present the frequency content corresponding to each temporal signal in the sample number domain, crucial for SVM feature extraction. (**a**) Temporal noisy signal SNR = 5 dB. (**b**) Temporal noisy signal SNR = 25 dB. (**c**) Scalogram SNR = 5 dB, plotted against sample numbers. (**d**) Scalogram SNR = 25 dB, plotted against sample numbers.

Numbered findings related to classification accuracy include the following:

1. The system achieved an average accuracy of 98.82% at SNR levels below 15 dB.
2. Precision and recall values remained consistently above 99% across all tested conditions.
3. A peak accuracy of 99.8% was observed at an SNR of 25 dB.

The system robustness was analyzed in detail and the results are given in Section 3.3.

3.2. Feature Extraction Efficacy

The CWT's application for feature extraction significantly enhanced the system's ability to distinguish between signal types, even in the presence of substantial noise and interference. The efficacy and selection of the wavelet parameters were instrumental in

optimizing the CWT for the specific application in underwater acoustic signal analysis. This subsection delves into the nuances of this optimization process.

3.2.1. Efficiency of the "Bump" Wavelet in Feature Extraction

The bump wavelet was chosen due to its structural affinity with the underwater acoustic signals of interest. Its ability to effectively decompose signals and extract salient features was paramount in the acoustically challenging underwater environment. Iterative testing and optimization of the "voices per octave" parameter within the MATLAB Wavelet Toolset underscored the importance of high-resolution analysis in effective feature extraction. The term voices per octave (VPOs) refers to the number of divisions within each octave of frequency when analyzing a signal. An octave represents a doubling in frequency, and more voices within an octave imply a finer resolution, which allows for a more detailed capture of signal nuances that are especially important in the varied and noise-prone underwater environment.

- **Iterative testing and parameter optimization**: A pivotal aspect of the methodological approach involved iterative testing and optimization of the "voices per octave" parameter within the MATLAB Wavelet Toolset. This parameter fine tuning was instrumental in enhancing the frequency resolution of the analysis, allowing for a nuanced examination of the signal characteristics at various scales.
- **Resolution impact and signal analysis performance**: Optimizing the VPO facilitated a high-resolution exploration of the signals, enabling the detection of intricate features that are often masked by noise or the signal transient nature. The bump wavelet performance, bolstered by the precise calibration of the VPO, underscored its effectiveness in the feature extraction process, thereby affirming its selection for the analysis carried out.

3.2.2. Impact of the Wavelet Parameters on the Signal Processing Outcomes

The selection and fine tuning of the wavelet parameters were pivotal in optimizing the CWT for underwater acoustic signal analysis. This subsection discusses the impacts of these parameters on the results and their significance in the feature extraction and classification processes.

- **VPO**: As above mentioned, this parameter dictates the resolution of the scale analysis within each octave. This parameter was adjusted to ensure that the CWT could discern subtle features within the acoustic signals, which could be critical for accurate classification and demodulation. A lower number of VPOs might gloss over these features, leading to a potential loss of critical information, while a higher value offers more granularity. To illustrate the impact of this parameter on the results, Figure 7 demonstrates how different settings affect the feature extraction and subsequent classification accuracy. A minimum of 35 voices per octave was determined as essential to capture the subtle nuances of the signals, underscoring the importance of high-resolution analysis in effective feature extraction.
- **Sample rate**: The sample rate, set at 2 MHz, was another significant parameter. It ensured that the detailed signal characteristics were preserved, allowing for an exhaustive analysis across the desired frequency ranges. This choice was instrumental in accommodating the wide bandwidth of underwater acoustic signals.
- **Frequency limits**: Setting frequency limits to focus on the 150 kHz to 250 kHz band allowed for concentrating the analysis on the most relevant parts of the signal. This targeted approach facilitated the extraction of pertinent features while excluding extraneous data, thereby enhancing the efficiency of the signal-processing pipeline.

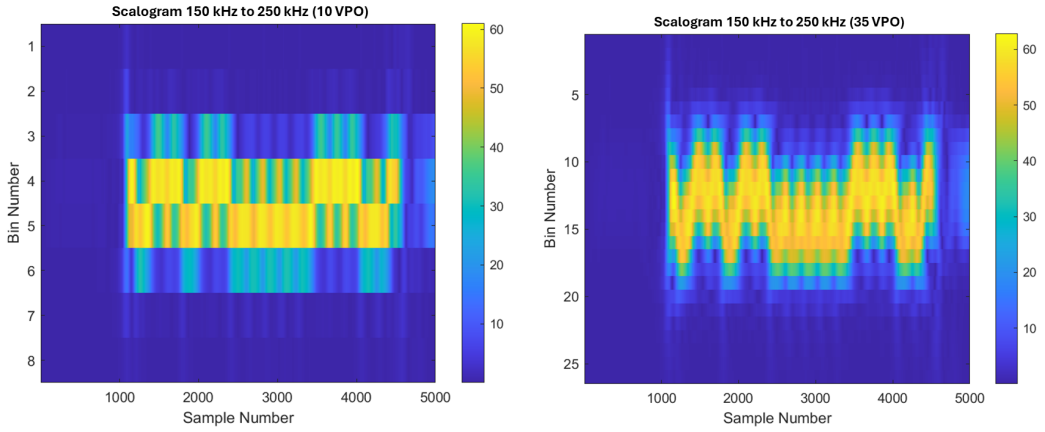

(**a**) (**b**)

Figure 7. Scalograms for low (10) and high (35) numbers of voices per octave. (**a**) Scalogram for VPO = 10. (**b**) Scalogram for VPO = 35.

3.3. Robustness Analysis of Signal Classification

The robustness of the developed SVM-based signal classification system was evaluated through a comprehensive noise analysis and a K-fold cross-validation to ensure its efficacy under different underwater acoustic conditions.

3.3.1. Noise Analysis

The resilience of the classification model against varying levels of environmental noise was a primary focus. Through extensive noise analysis, the model demonstrated very good performance, maintaining high accuracy even in high-noise scenarios (see Table 1). The different SNR levels were simulated with additive white Gaussian noise incorporated into the transmitted signal. This attribute is crucial for underwater acoustic communications, where noise levels can significantly impact the signal integrity. The model classification accuracy across a broad spectrum of SNR levels was assessed, ensuring its applicability in real-world underwater environments.

3.3.2. K-Fold Cross-Validation

To further validate the reliability of the classification system, K-fold cross-validation techniques were employed. This approach not only provided a robust evaluation of the model performance but also eliminated bias by ensuring that the model was tested across multiple subsets of the data. The K-fold validation results underscored the model's consistent accuracy and its capacity to generalize well across unseen data, which is vital for deploying the system in diverse underwater conditions (see Table 3).

The findings from both the noise analysis and K-fold validation experiments affirmed the robustness of the signal classification approach. Notably, the model's ability to retain high classification accuracy across different noise levels and validation subsets demonstrated its potential for reliable application in underwater acoustic signal processing tasks.

Table 3. Accuracy for each fold in the K-fold cross-validation process.

Fold 1	Fold 2	Fold 3	Fold 4	Fold 5	Fold 6	Fold 7	Fold 8	Fold 9	Fold 10
1.0000	1.0000	1.0000	1.0000	1.0000	1.0000	1.0000	1.0000	1.0000	0.9980

3.4. Performance Analysis

This section delineates the performance metrics of the developed SVM-powered underwater modem system, with a focus on its demodulation capabilities. Through rigorous experimentation, the system demonstrated very good performance in terms of

signal classification accuracy, robustness in various noise conditions, and a consistent demodulation bitrate, which are critical factors for effective underwater communication.

- Accuracy and robustness: The demodulation process accuracy was evaluated across a spectrum of SNR levels, with the model exhibiting an impressive accuracy of 98.28%, even at a low SNR of 5 dB. As the SNR increased, the accuracy ascended, peaking at 99.78% for SNRs of 23, 24, and 25 dB, indicating the high fidelity of the system in signal reconstruction under diverse noise conditions. This robustness is crucial, as it directly relates to a lower bit error rate (BER), which is a key determinant of the demodulation success in real-world underwater communication systems.
- Precision and recall: The precision and recall metrics further substantiate the demodulation efficacy. Precision quantifies the proportion of true positives against all positive predictions, and recall measures the proportion of true positives identified correctly. At the highest tested SNR of 25 dB, the precision and recall for class "1" were 99.79% and 99.39%, respectively, and for class "0", both metrics were 99.90%. These high values suggest that the system correctly demodulated the FSK signals, which is indicative of an extremely low BER, and thus, high data integrity.
- Demodulation bitrate: beyond these classification metrics, the system achieved a stable and consistent demodulation bitrate of 10,000 bauds.

Beyond the metrics of precision and recall, the main point of the demodulation strategy hinges on the unique processing of symbols, where each "1" or "0" and the transitional "C" symbol was distinctly represented by 100 digitized samples. This precise sample-based representation facilitated an accurate symbol identification and boundary delineation process. By systematically analyzing the output from the SVM, which decided the start and end points of each symbol, the system ensured that the integrity of the transmitted data was maintained. As a result, a demodulation bitrate of 10,000 bauds was achieved, with the final demodulated symbols reflecting a BER of zero. This outcome not only validated the robustness of the SVM-powered modem but also possibly set a new standard in the fidelity of underwater communication systems. This zero BER is a testament to the precision achieved, confirming the system capability to deliver flawless data transmission under controlled experimental conditions.

4. Discussion

In the preliminary phases of this research, the fast Fourier transform (FFT) was employed for transforming time-domain signals into their frequency-domain representations. However, significant challenges were encountered due to the non-periodic nature of the underwater acoustic signals and their non-zero starting points. This resulted in frequency (energy) leakage, thereby complicating the accurate analysis of these signals.

The short-time Fourier transform (STFT) presented an alternative with its time-frequency representation capabilities. Despite its promise, the STFT was confronted with limitations related to the dimensionality and resolution. It generated a considerably larger set of features (52 bins) compared with the more efficient CWT, which produced only 11 features. This efficiency made the CWT a more suitable choice for feature extraction within the constraints and goals of the underwater signal analysis. The main advantages of the CWT can be summarized as follows:

- Time–frequency localization: Contrary to the FFT/DFT, which provide purely frequency-domain information, and the STFT, which offers a rudimentary time–frequency analysis, the CWT yields a nuanced and continuous time–frequency representation of signals. This is especially beneficial for analyzing non-stationary signals or those with time-varying characteristics prevalent in underwater communication.
- Flexibility in feature extraction: The ability of the CWT to analyze signals across all possible scales affords unmatched flexibility in capturing transient or rapidly evolving features within signals. This adaptability was crucial for identifying nuanced features in modulated underwater signals, which could not be adequately captured by the fixed and dyadic scales of the DWT or the limited resolution of the STFT.

- Dimensionality and computational efficiency: By extracting a reduced number of features (11 features with the CWT) compared with the STFT approach (52 bins), the classification process was significantly streamlined, enhancing computational efficiency without sacrificing the depth of the signal representation.
- Overcoming limitations of Fourier transform methods: The CWT approach to signal analysis effectively addressed the challenges of frequency leakage and the analysis of non-periodic underwater acoustic signals, which greatly complicated the use of traditional FFT/DFT methods.

This comparative analysis underscores the transformative potential of the CWT in overcoming the intrinsic limitations of Fourier transform methods, particularly in the complex realm of underwater acoustic signal processing.

In the development of the classification model, a remarkable synergy emerged from the combination of the SVM, CWT, and strategic inclusion of the "C" symbol as a delimiter between characters. This innovative approach was shown to be instrumental in achieving exceptional robustness and reliability in signal classification, eliminating the immediate need for the Reed–Solomon error correction techniques typically employed to enhance signal integrity. Notably, misclassifications involving the "1" or "0" symbols consistently occurred with an adjacent "C" symbol, primarily at the boundaries of signal sequences. This observation is crucial, as it underscores the absence of direct misclassifications between "1" and "0", effectively minimizing the potential for error in critical signal interpretation. The "C" symbol serves as a robust buffer, significantly reducing ambiguity and ensuring high precision in the classification of "1" and "0". Thus, the strength of the model lies not merely in its high precision and recall metrics but in its fundamental design, which leverages the "C" symbol to navigate the complexities of underwater acoustic signal processing. This strategic choice highlights the model's innovative edge, offering a powerful testament to its capacity to deliver reliable classifications without the immediate recourse to traditional error correction strategies.

Regarding the key performance metrics previously mentioned in Section 3, they can be summarized as follows:

- Data transmission rate: The system achieved a remarkable data transmission rate of 10,000 bauds, which is capable of processing 1 bit every 100 microseconds. This metric is especially significant given the high-noise environments typical of underwater communication.
- Noise resilience: At a low SNR of just 5 dB, the system demonstrated exceptional resilience, maintaining an accuracy of 98.28%. This resilience is indicative of the robustness of the approach, which effectively handled the substantial noise levels that often compromise other communication systems.
- Future enhancements: There is considerable potential for incorporating Reed–Solomon error correction to further enhance the reliability. This addition would capitalize on the system's ability to handle errors and improve the data integrity without the complexity of additional hardware.

By establishing these benchmarks, this study not only demonstrated the high performance of the current system but also set the stage for future innovations in underwater acoustic communication. The metrics provided served not just as evidence of the system effectiveness but as a foundation for ongoing improvements and adaptations.

5. Conclusions

This study successfully demonstrated the application of support vector machines and the continuous wavelet transform for signal classification and feature extraction, respectively, in underwater acoustic communication. The findings emphasize the potential of machine learning in enhancing signal processing techniques under challenging conditions, such as those found in underwater environments. The work presented in this paper pioneered the application of the CWT for feature extraction and an SVM for demodulating FSK underwater acoustic signals over an FPGA-based architecture. This approach represents

a significant departure from traditional methods, which have predominantly focused on modulation-type identification rather than the complete demodulation process.

Therefore, the present research contributed a new methodology to the field of underwater acoustic communication by employing an SVM not just for the identification of modulation types but also for the demodulation of signals. This distinction should open new pathways for the development of advanced underwater communication systems because it is believed that this could lay the groundwork for future advancements in underwater communication by enhancing signal robustness, reducing energy consumption, and improving data transmission efficiency.

Future research directions point to enhancing the robustness and efficiency of underwater communication systems. The exploration of Solomon–Reed encoding presents a promising research line for improving the signal robustness, while the potential reduction in the number of cycles per symbol offers positive prospects for energy conservation. Additionally, replacing the conventional "clock" or "reference" signal with a chirp signal could provide a more reliable means for synchronization and signal detection in multipath underwater environments.

Author Contributions: Conceptualization, G.S.G.-C.; methodology, G.S.G.-C.; software, G.S.G.-C.; validation, G.S.G.-C., D.M.-S. and J.S.-M.; formal analysis, G.S.G.-C.; investigation, G.S.G.-C., D.M.-S. and J.S.-M.; resources, G.S.G.-C.; data curation, G.S.G.-C.; writing—original draft preparation, G.S.G.-C., D.M.-S. and J.S.-M.; writing—review and editing, G.S.G.-C., D.M.-S. and J.S.-M.; visualization, G.S.G.-C., D.M.-S. and J.S.-M.; supervision, D.M.-S. and J.S.-M.; project administration, D.M.-S. and J.S.-M.; funding acquisition, D.M.-S. and J.S.-M. All authors read and agreed to the published version of the manuscript.

Funding: This work was supported in part by the "Ministerio de Ciencia e Innovación" of Spain under project PID2020-112658RBI00/10.13039/501100011033 and project PID2020-112502RB-C44. Part of this work was also supported by Innovation Group "IEData" GID2016-6.

Institutional Review Board Statement: Not applicable.

Informed Consent Statement: Not applicable.

Data Availability Statement: All materials, data, computer code, and protocols associated with this study are available upon reasonable request to the authors. Efforts have been made to ensure that all components of the study are reproducible and accessible to interested researchers. Specific details on the hardware components and software codes can be provided by the corresponding author. Datasets generated and analyzed during the current study are available from the corresponding authors upon reasonable request. These datasets include raw signal captures, processed data, and classification results, all of which are integral to replicating the study's findings.

Conflicts of Interest: The authors declare no conflicts of interest.

Abbreviations

The following abbreviations are used in this manuscript:

UWA	Underwater acoustic
FPGA	Field-programmable gate array
CWT	Continuous wavelet transform
SVM	Support vector machine
FSK	Frequency shift keying
ASK	Amplitude shift keying
PSK	Phase shift keying
ICI	Intercarrier interference
CNN	Convolutional neural networks
DWT	Discrete wavelet transform
BPSK	Binary phase shift keying
QPSK	Quadrature phase shift keying
AFSK	Asymmetric frequency shift keying

VLC	Visible light communication
DCNN	Deep convolutional neural network
DL	Deep learning
SNR	Signal-to-noise ratio
RBF	Radial basis function
CV	Cross-validation
VPO	Voice per octave
BER	Bit error rate
FFT	Fast Fourier transform
DFT	Discrete Fourier transform
STFT	Short-time Fourier transform

References

1. Ali, M.; Khan, A.; Bertozzi, M.; Ullah, U.; Altowaijri, S.M.; Ali, I.; Iqbal, S.; Alamoodi, A. Energy and Path-Aware-Reliable Routing in Underwater Acoustic Wireless Sensor Networks. *Wirel. Commun. Mob. Comput.* **2022**, *2022*, 8535244. [CrossRef]
2. Moreno-Salinas, D.; Pascoal, A.; Aranda, J. Optimal Sensor Placement for Acoustic Underwater Target Positioning With Range-Only Measurements. *IEEE J. Ocean. Eng.* **2016**, *41*, 620–643. [CrossRef]
3. Junejo, N.U.R.; Esmaiel, H.; Sattar, M.; Sun, H.; Khalil, M.A.; Ullah, I.; Wen, M. Sea Experimental for Compressive Sensing-Based Sparse Channel Estimation of Underwater Acoustic TDS-OFDM System. *Wirel. Commun. Mob. Comput.* **2022**, *2022*, 2523196. [CrossRef]
4. Asharjabi, S.; Sakran, H.; Al-nahari, A.; Esmaiel, H. Time-Domain Channel Estimation Scheme for OFDM over Fast Fading Channels. *Wirel. Commun. Mob. Comput.* **2022**, *2022*, 7839430. [CrossRef]
5. Qasem, Z.A.H.; Leftah, H.A.; Sun, H.; Esmaiel, H.; Basit, A. Precoded IM-OFDM-SS for Underwater Acoustic Communication. *Wirel. Commun. Mob. Comput.* **2022**, *2022*, 7940993. [CrossRef]
6. Zhu, Y.; Wang, B.; Xie, F.; Wu, C.; Chao, P.; Bazzi, A. Data-Driven Signal Detection for Underwater Acoustic Filter Bank Multicarrier Communications. *Wirel. Commun. Mob. Comput.* **2022**, *2022*, 4943442. [CrossRef]
7. Gao, D.; Hua, W.; Su, W.; Xu, Z.; Chen, K.; Esmaiel, H. Supervised Contrastive Learning-Based Modulation Classification of Underwater Acoustic Communication. *Wirel. Commun. Mob. Comput.* **2022**, *2022*, 3995331. [CrossRef]
8. Rahman, M.H.; Shahjalal, M.; Hasan, M.K.; Ali, M.O.; Jang, Y.M. Design of an SVM Classifier Assisted Intelligent Receiver for Reliable Optical Camera Communication. *Sensors* **2021**, *21*, 4283. [CrossRef] [PubMed]
9. Luo, H.; Xu, Z.; Wang, J.; Yang, Y.; Ruby, R.; Wu, K.; Zhang, X. Reinforcement Learning-Based Adaptive Switching Scheme for Hybrid Optical-Acoustic AUV Mobile Network. *Wirel. Commun. Mob. Comput.* **2022**, *2022*, 9471698. [CrossRef]
10. Gorday, P.E. Machine Learning Demodulator Architectures for Power-Limited Communications. Ph.D. Thesis, Florida Atlantic University, The College of Engineering and Computer Science, Boca Raton, FL, USA, 2020.
11. Dormido-Canto, S.; Vega, J.; Sánchez, J.; Farias, G. Information Retrieval and Classification with Wavelets and Support Vector Machines. In *Artificial Intelligence and Knowledge Engineering Applications: A Bioinspired Approach*; Mira, J., Álvarez, J.R., Eds.; Springer: Berlin/Heidelberg, Germany, 2005; pp. 548–557.
12. Zhang, Q. Signal Classification Implemented by Wavelet Analysis and Support Vector Machine. Master's Thesis, University of Gävle, Faculty of Engineering and Sustainable Development, Gävle, Sweden, June 2013.
13. Hazza, A.; Shoaib, M.; Saleh, A.; Fahd, A. A novel approach for automatic classification of digitally modulated signals in HF communications. In Proceedings of the 10th IEEE International Symposium on Signal Processing and Information Technology, Luxor, Egypt, 15–18 December 2010; pp. 271–276. [CrossRef]
14. Keshk, M.E.; Amartuvshin, D.; Rodriguez, R.; Asami, K. Design SVM Classifier for Automatic Modulation Recognition Systems. *UNISEC Space Takumi J. Pract. Study Probl. Find. Solving Space Syst.* **2018**, *7*, 1–14.
15. Sadiq, M.W.; Kabir, M.A. Design and implementation of reconfigurable ASK and FSK modulation and demodulation algorithm on FPGA (Field Programmable Gate Array). *Sens. Int.* **2022**, *3*, 100155. [CrossRef]
16. Yamga, G.M.; Ndjiongue, A.R.; Ouahada, K. Low complexity clipped Frequency Shift Keying (FSK) for Visible Light Communications. In Proceedings of the 2018 IEEE 7th International Conference on Adaptive Science & Technology (ICAST), Accra, Ghana, 22–24 August 2018; pp. 1–6. [CrossRef]
17. Mohammad, A.S.; Reddy, N.; James, F.; Beard, C. Demodulation of faded wireless signals using deep convolutional neural networks. In Proceedings of the 2018 IEEE 8th Annual Computing and Communication Workshop and Conference (CCWC), Las Vegas, NV, USA, 8–10 January 2018; pp. 969–975. [CrossRef]
18. Daldal, N.; Sengur, A.; Polat, K.; Cömert, Z. A novel demodulation system for base band digital modulation signals based on the deep long short-term memory model. *Appl. Acoust.* **2020**, *166*, 107346. [CrossRef]
19. Wang, H.; Wu, Z.; Ma, S.; Lu, S.; Zhang, H.; Ding, G.; Li, S. Deep Learning for Signal Demodulation in Physical Layer Wireless Communications: Prototype Platform, Open Dataset, and Analytics. *IEEE Access* **2019**, *7*, 30792–30801. [CrossRef]
20. Huang, X.; Li, X. Modulation identification method based on time-frequency analysis and support vector machine. In Proceedings of the 2023 IEEE 2nd International Conference on Electrical Engineering, Big Data and Algorithms (EEBDA), Changchun, China, 24–26 February 2023; pp. 551–554. [CrossRef]

21. Zhang, X.; Ge, T.; Chen, Z. Automatic Modulation Recognition of Communication Signals Based on Instantaneous Statistical Characteristics and SVM Classifier. In Proceedings of the 2018 IEEE Asia-Pacific Conference on Antennas and Propagation (APCAP), Auckland, New Zealand, 5–8 August 2018; pp. 344–346. [CrossRef]
22. Hamee, H.M.; Wadi, J. Automatic Modulation Recognition for MFSK Using Modified Covariance Method. *Int. J. Electr. Comput. Eng. (IJECE)* **2015**, *5*, 429–435. [CrossRef]
23. Zhou, X.; Wu, Y.; Yang, B. Signal Classification Method Based on Support Vector Machine and High-Order Cumulants. *Wirel. Sens. Netw.* **2010**, *2*, 48–52. [CrossRef]
24. Makili, L.; Vega, J.; Dormido-Canto, S. Incremental support vector machines for fast reliable image recognition. *Fusion Eng. Des.* **2013**, *88*, 1170–1173. [CrossRef]
25. Weimin, Z.; Daoying, P. SVM with linear kernel function based nonparametric model identification and model algorithmic control. In Proceedings of the 2005 IEEE Networking, Sensing and Control, Tucson, AZ, USA, 19–22 March 2005; pp. 982–987. [CrossRef]
26. Keogh, E.; Chakrabarti, K.; Pazzani, M.; Mehrotra, S. Dimensionality Reduction for Fast Similarity Search in Large Time Series Databases. *Knowl. Inf. Syst.* **2001**, *3*, 263–286. [CrossRef]
27. Dormido-Canto, S.; Farias, G.; Dormido, R.; Vega, J.; Sánchez, J.; Santos, M.; TJ-II-Team. TJ-II wave forms analysis with wavelets and support vector machines. *Rev. Sci. Instrum.* **2004**, *75*, 4254–4257. [CrossRef]